Microfluid Nanofluid (2013) 14:831–838
DOI 10.1007/s10404-012-1094-4

ORIGINAL ARTICLE

Trajectory shift of magnetic microchains in an oscillating field

Yan-Hom Li · He-Ching Lin · Ching-Yao Chen

Received: 31 August 2012 / Accepted: 4 November 2012 / Published online: 22 November 2012

Abstract We report an interesting phenomenon of "trajectory shift" of magnetic chains in an oscillating field, when the phase angle lags of chains to the external field exceeding 90°. The phenomenon shifts the oscillating trajectory of chain along a new axis, which is perpendicular to its original axis. Applicability of the phenomenon to a stable chain in various conditions is experimented systematically. The trajectory shift provides an effective manipulating mechanism in micro-electro-mechanical-systems, such as steering of micro-swimmers. We successfully demonstrate that the driven direction of a micro-swimmer can be controlled by shifting its oscillating trajectory without a physical re-configuration of the external field.

Keywords Magnetic particle · Micro-chain · Trajectory shift · Micro-swimmer · Steering mechanism

1 Introduction

Magnetorheological (MR) suspension, an artificial and smart fluid consisting of paramagnetic solid particles suspended in a nonmagnetic solvent, has been actively studied and applied in the so-called magnetofluidics (Nguyen 2012). A remarkable class of this smart material is the ferrofluid, whose particles are nanometer-sized and coated by surfactants (Rosensweig 1985). Applications of ferrofluid in multistage rotary seals, inertial dampers, and loudspeakers had been well-established in the industry (Rosensweig 1985). New applications are implemented in the domain of micro-technology as reported in a recent review by Nguyen (2012). In addition, due to its visual appeal and prompt response to magnetic stimuli, this fluid material has become an archetypal dipolar system for the study of a number of pattern-forming processes in engineering and science, i.e., in a perpendicular field (Chen et al. 2008, Chen and Li 2010) and a radial field (Chen et al. 2009, 2010), or even in arts (Kodama 2008).

On the other hand, micrometer-sized magnetic beads contained in MR suspension are applicable to reversible devices in micro-electro-mechanical-systems (MEMS), such as micro-mixers (Biswal and Gast 2004a; Kang et al. 2007; Roy et al. 2009; Martin et al. 2009), micro-swimmers (Dreyfus et al. 2005; Ghosh and Fischer 2009; Li et al. 2012a), and other microfluidics (Terray et al. 2002; Gijs 2004; Nguyen 2012). Among the micro-mixing devices, a popular way is manipulating the chained beads in a dynamical magnetic field, such as a rotational field (Biswal and Gast 2004a, b; Kang et al. 2007; Roy et al. 2009), or a so-called vortex magnetic field (Martin et al. 2009). Detailed dynamics regarding the chaining process of beads as well as motion of the micro-chain in a rotating field have been studied extensively in the last decade, including experiments (Melle et al. 2000, 2002a, b; Vuppu et al. 2003) and simulations (Kang et al. 2007; Petousis et al. 2007). It is concluded that the governing parameters of such a rotating chain are the dimensionless Mason number (Melle and Martin 2003; Melle et al. 2003), which determines the ratio between the magnetic force and the hydrodynamic drag, as well as the number of particles contained in the chain. When these parameters exceed certain critical values, structural rupture occurs within the early transient time period, mainly near the center of the chain (Melle and Martin 2003; Petousis et al. 2007).

Y.-H. Li · H.-C. Lin · C.-Y. Chen (✉)
Department of Mechanical Engineering,
National Chiao Tung University, Hsinchu, Taiwan, ROC
e-mail: chingyao@mail.nctu.edu.tw

Nevertheless, the positions of the fracture might relocate due to variations in bead susceptibility. In addition, depending on the permeability of the particles, either a brittle or a ductile chain fracture is possible (Melle and Martin 2003). The critical length to prevent a rupture is proposed to be inversely proportional to the square root of the Mason number (Melle and Martin 2003).

A similar problem dealing with micro-chains in an oscillating field has drawn much less attention. Compared to the condition in a rotational field, understandings of an oscillating chain are more challenging due to its strong transient phenomena, for instance, significant variation of angular speed and field strength within a period of oscillation. Nevertheless, the incorporation of such an oscillating field in a MEMS or Lab-on-a-Chip is rather straightforward (Petousis et al. 2007; Lacharme et al. 2009; Weddemann et al. 2011; Karle et al. 2011; Wittbracht et al. 2012). In addition, an oscillating micro-chain consisted of magnetic beads with different sizes has been successfully implemented to mimic a micro-swimmer. Dreyfus et al. (2005) connected micrometer-sized superparamagnetic beads by nanometer-sized DNA to provide stronger inter-particle bonding forces. The chain was then attached to a larger biological red blood cell, and manipulated in an oscillating field to move forward. Li et al. (2012a) created re-dispersible artificial micro-swimmers by simply chaining superparamagnetic beads of different sizes. Sufficient propulsion can be generated to drive the swimmers moving forward. However, the efficiencies of their artificial swimming devices are much lower than natural swimmers. In the follow-up study (Li et al. 2012b), detailed dynamics of oscillating chains are discussed, including synchronicity of the phase angle trajectories between the oscillating chains and the external fields as well as the influences of the control parameters. A criterion leading to structural fracture is proposed based on the experimental validations.

In this paper, an interesting phenomenon of inconsistent motion of a magnetic chain with the external oscillating field, referred to as the "trajectory shift", is reported and experimented systematically. To highlight the great potential applications of the trajectory shift phenomenon in the MEMS, steering of a micro-swimmer is demonstrated.

2 Experimental setup

The experimental configuration is schematically demonstrated in Fig. 1, which is mostly identical to what had been used in Li et al. (2012a, b). Micrometer-sized magnetic particles are initially dispersed in distilled water. The magnetic particles used in the experiments are aqueous superparamagnetic polystyrene microspheres coated with iron oxide grains produced by Invitrogen Life Tech. The

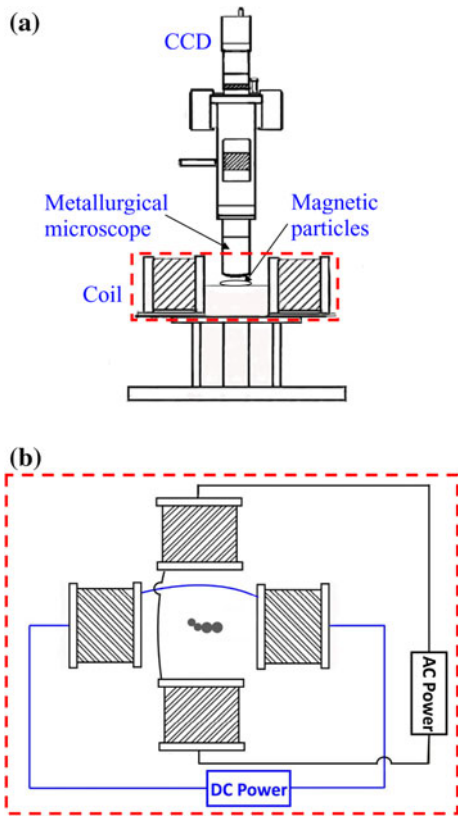

Fig. 1 **a** Schematic of experimental setup, and **b** top view configuration of coil pairs for generation of oscillating magnetic field. The size of the oscillating particle chain in **b** is exaggerated and not in actual scale

mean radii of the microspheres (denoted as a) are $a = 2.25$ and 1.4 μm, with a susceptibility of $\chi = 1.6$ and no magnetic hysteresis or remanence. The magnetization of particles is saturated to the value of 375 G in a field strength greater than 10,000 Oe. All the experiments are conducted under the field strengths less than 200 Oe to preserve a near linearity between the magnetization and the external field. The micrometer sizes of magnetic beads prevent from the influences of random Brownian motion, so the system can be effectively manipulated by the external field.

A static unidirectional magnetic field, denoted as H_d, is generated first by a pair of coils powered by DC power sources. Magnetic particles magnetized by the directional field tend to aggregate and form chains because of dipolar attractive forces. It is noticed that the experiments are conducted in a dilute condition, so that the interference between the manipulated chain and other isolated particles or chains is minimized. To create an oscillating field, another pair of coils are placed perpendicularly to the former pair and connected to AC power supplies to generate a sinusoidal dynamical perpendicular field (H_v) with a maximum field strength H_p and frequency f, i.e. $H_v = H_p \sin(2\pi ft)$. This additional perpendicularly dynamical field

and the original static directional field result in an overall oscillating field ($\vec{H}$) of $\vec{H} = H_d\vec{i} + H_v\vec{j}$, in which i and j are unit vectors in the directional and perpendicular axis, respectively. Under such a field configuration, the phase angle trajectory (θ) of the external field, which represents the angle between orientations of the instantaneous overall field and the directional field, is prescribed as $\theta(t) = \tan^{-1}[(H_p/H_d)\sin(2\pi ft)]$ associated with an amplitude (denoted as θ_{Amax}) of $\theta_{Amax} = \tan^{-1}(H_p/H_d)$. The magnetic particle chain, which tends to align along the orientation of the external field, would oscillate under the presence of such an oscillating field. The motion of the particle chain is recorded by an optical microscope connected to a digital camera (Silicon Video 643C) whose maximum shooting rate is 200 frames/s. The recording system is incorporated with an image software (Ulead GIF Animator) to display snapshot images every 1/30 s for further analysis. Representative snapshot images, which are modified from the original recorded movies by improving their contrasts and resolutions, are presented in the following sections to identify the distinct behaviors of particle chains under various conditions.

3 Results and discussion

3.1 Trajectory shift of an oscillating chain

It has been demonstrated that a paramagnetic chain oscillates along the external field (Li et al. 2012a, b). For readers' easier references, Fig. 2 shows a similar case of a chain consisted of eight particles (denoted as a P8 chain) subjected to an oscillating field configuration of $H_d = 24.15$ Oe, $H_p = 56.68$ Oe, and $f = 1$ Hz (or oscillating period $P = 1$ s) within one and a half oscillating periods, i.e., $0 \le t \le 3P/2$. Under such a field condition, the chain behaves as a rigid beam and oscillates nearly concurrently with the external field, i.e., counter-clockwise at $t < P/4$ and $3P/4 < t < 5P/4$, clockwise at $P/4 < t < 3P/4$ and $5P/4 < t < 3P/2$. The trajectories of phase angle (denoted as θ), extended to two full oscillating periods, of the external field and the chain are constructed accordingly and shown in Fig. 3. Consistent with early studies (Li et al. 2012b), the magnitudes of instantaneous phase angle lag (denoted as $\Delta\theta_L$ and defined in Fig. 2) are not that large in the present situation, except near the timings at $t = P/2$, P, $3P/2$, when the perpendicular component of the overall field vanishes and results in very significant angular accelerations locally. After an initial transient stage caused by the sudden start, both the frequency and amplitude of the oscillating trajectory of the chain reveal close similarities to the external field. More detailed discussions regarding the concurrently oscillating chain are referred to Li et al. (2012b).

The early investigations by Li et al. (2012a, b)mainly focused on either stable chains under moderate field strengths or structural failures in excessive strengths. If the condition is modified to maintain a stable chain under a significant perpendicular field strength, e.g., $H_p = 176.13$ Oe, an interesting phenomenon of local inconsistent motion between the chain and the field is observed as shown in Fig. 4. By inspecting the sequential images in Fig. 4,

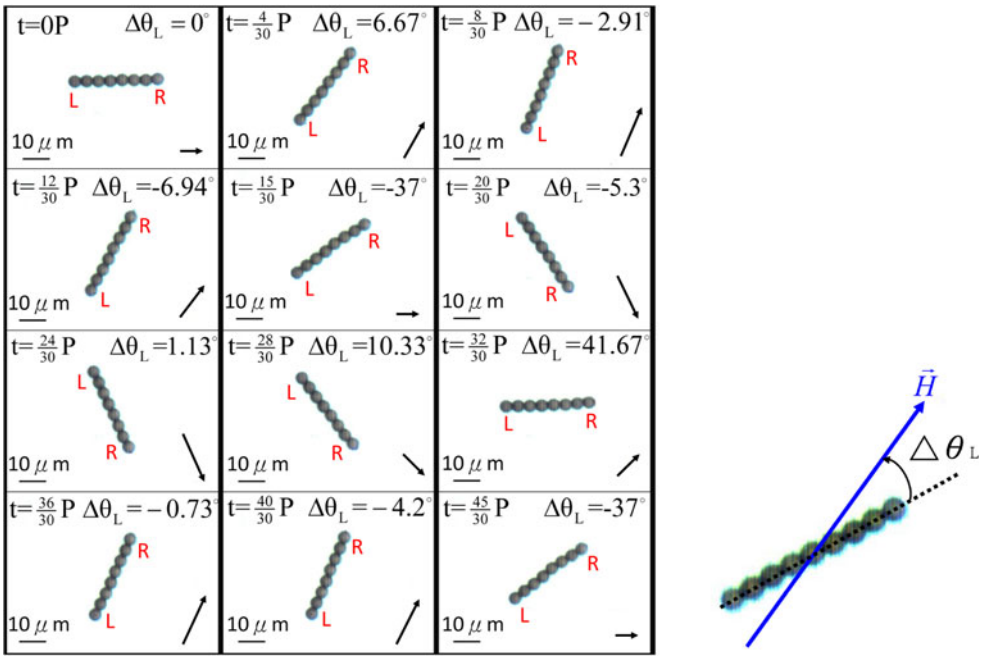

Fig. 2 Images of an 8-particle (P8) chain oscillating under the field configuration of $H_d = 24.15$ Oe, $H_p = 56.68$ Oe, and $f = 1$ Hz. The lengths and orientation of *black arrows inside images* represent the strength and orientation of the instantaneous overall field, respectively. In the present condition, the magnetic chain oscillates along the external field but lags behind by insignificant phase angles (denoted as $\Delta\theta_L$) except near the timings when the perpendicular field vanishes at $t = P/2$, P, $3P/2$

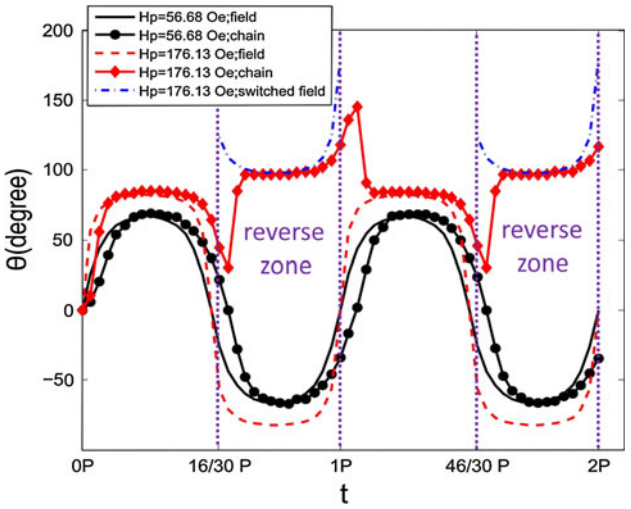

Fig. 3 Trajectories of the phase angle (θ) of a P8 oscillating chain and its corresponding external field of constant $H_d = 24.15$ Oe and $f = 1$ Hz in different perpendicular field strengths of $H_p = 56.68$ and 176.13 Oe. The oscillating trajectory of the chain subjected to a weaker perpendicular field of $H_p = 56.68$ Oe follows the external field closely. Because of the excessive phase lag of $|\Delta\theta_L| > 90^o$ at $t = 17P/30$, $47P/30$ in the case of $H_p = 176.13$ Oe, interesting reverse motion of the oscillating chain is observed, referred to as a phenomenon of "trajectory shift". An alternative to describe of the trajectory shift is viewing as if the polar orientations of the external field are switched. The phase trajectory of the imaginary "switched field" is 180° greater than the original one as displayed by the *dash–dot lines*. During the time of reverse motion, the chain follows a nearly identical trajectory of the imaginary "switched field"

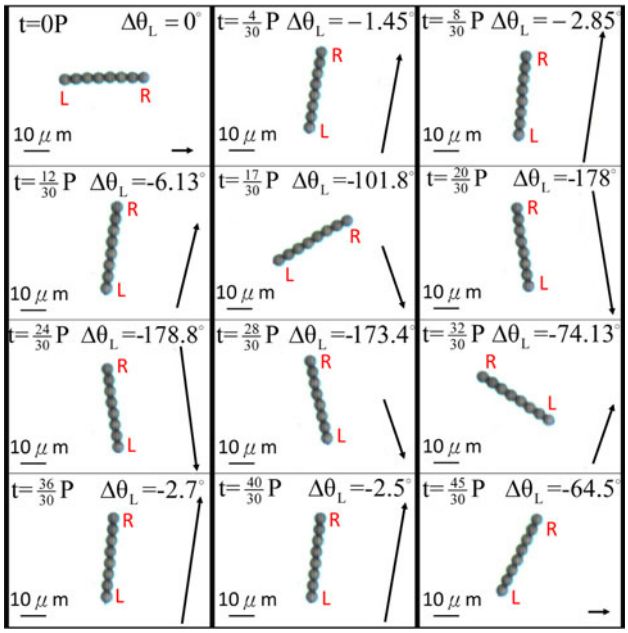

Fig. 4 Images of 8-particle (P8) chain oscillating under a stronger field configuration of $H_d = 24.15$ Oe, $H_p = 176.13$ Oe, and $f = 1$ Hz. Because of the instantaneous excessive phase lag of $|\Delta\theta_{Lmax}| > 90°$, instead of an oscillation along the horizontal axis shown in Fig. 2, the chain oscillates reversely along the perpendicular axis within $17P/32 < t < 32P/30$

instead of a concurrent oscillation with the external field, i.e., clockwise at $17P/30 < t < 20P/30$, the chain rotates reversely (counter-clockwise). Afterward, the chain oscillates along the perpendicular axis (or $\theta = 90^o$), rather than the original horizontal axis of the external field (or $\theta = 0^o$). The reverse motion can be observed more clearly by the phase angle trajectory shown in Fig. 3. At $t = 17P/30$, an apparent phase trajectory shift of the chain can be identified. Consequently, trajectory of the chain completely deviates from the external field during the time at $17P/30 < t < 32P/30$. The chain changes its oscillating orientation dramatically at about $t = 33P/30$ and resumes to follow the original trajectory of the external field until the occurrence of the second reverse motion at $t = 47P/30$. Excluding the initial start at $t < 4P/30$, a distinct pattern of oscillation along the perpendicular axis of $\theta = 90^o$ is resulted, which is referred to as "trajectory shift" thereafter.

The mechanism of the trajectory shift can be understood by the induced magnetic torque. It is well concluded that the motion of a magnetic chain is dominated by the competition between induced hydrodynamic drags and the magnetic forces, which is defined as a dimensionless Mason number (Mn). When a chain composed of N particles is subjected to a rotational field, the chain experiences a magnetic torque (M^m) and an opposing viscous drag (M^v) given as (Melle et al. 2003; Biswal and Gast 2004b; Roy et al. 2009)

$$M^m = \frac{\mu_0 \mu_s}{4\pi} \frac{3|\vec{m}|^2 N^2}{2(2a)^3} \sin(2\Delta\theta_L) \tag{1}$$

$$M^v = \frac{4}{3} N\pi a^3 \frac{2N^2}{\ln(N/2)} \eta\omega \tag{2}$$

$$Mn = \frac{32\eta\omega}{\mu_0 \chi^2 \left|\vec{H}\right|^2} \tag{3}$$

Here μ_0 and μ_s stand for the vacuum permeability and the relative permeability of the solvent, respectively. $\vec{m}$ is the dipole moment of a magnetic particle, and η is the viscosity of the solvent fluid. The angular speed of the chain and the magnitude of the overall external field strength are expressed as ω and $\left|\vec{H}\right|$, respectively. It is noticed that ω and $\left|\vec{H}\right|$ vary with time within the oscillations, so that the Manson number is also time-dependent, i.e., Mn(t), which is distinct from the conventional rotational microchains.

In general, the chain oscillates more synchronized with the external field, i.e., smaller phase lags, under a stronger perpendicular field strength. Nevertheless, as mentioned above the instantaneous phase lags increase dramatically in

the vicinity at $t = P/2$, P, $3P/2$ due to the significant acceleration of angular speed locally, e.g., figure 7b in Li et al. (2012b). By the same token, the present field strength results in the instantaneous phase lag of $\Delta\theta_L = -101.8°$ at $t = 17P/30$ as shown in Fig. 3. According to Eq. (1), the magnetic torque changes its sign at 90° multiples of the phase lag, so that the chain would start to be pulled oppositely to the external field, i.e., counter-clockwise, when $|\Delta\theta_L| > 90°$. Nevertheless, when the lagging phase angle reduces to $|\Delta\theta_L| < 90°$ after $t = 32P/30$, the magnetic torque changes sign again, and the chain resumes to its original oscillating trajectory. As a result, two dramatic shifts of the phase trajectory are observed within one oscillating period as shown in Fig. 3. Similar scenarios would occur periodically afterward and result in a distinct pattern of oscillation.

This reserve oscillation can also be explained physically by paramagnetism of the chain. By the paramagnetic features, the orientations of induced magnetic poles of the chain would point toward the same direction with the external field, marked by arrow in the images, in a static condition at $t = 0$ shown in Fig. 4. In another word, the North Pole is located at right endpoint of the chain which is marked by "R" in the images. Under a dynamical field condition, the instantaneous movement of the external field causes a lagging angle and induces the poles to re-orientate toward the field. If the instantaneous field shift is not too dramatic, such as the situation of $|\Delta\theta_L| < 90°$ at $t < 12P/30$, the orientation of induced poles of the chain would tend to catch up the external field. However, in a condition of $|\Delta\theta_L| > 90°$ as shown at $t = 20P/30$, the left endpoint of the chain is now physically closer to the North Pole of the external field. Consequently, the induced poles would switch their locations, so that the North Pole switches from location at "R" to "L". By the same token, the induced poles would switch back to their original locations when the right endpoint of chain is again closer to the North Pole of the external field at $t = 32P/30$. The continuing switches of induced poles lead to the trajectory shifts (or reverse oscillation) periodically.

An alternative to qualitatively assess the effects of pole-switch of the chain is viewing as if the orientation of the external field is switched, but not the induced poles. The phase trajectory of the imaginary "switched field" would be 180° greater than the original one during the time interval of reverse motion. Trajectory of this "switched field" is also plotted in Fig. 3. Both trajectories of the chain and the "switch field" collapse nicely during the time interval of trajectory shift at $19P/30 < t < 28P/30$. After $t > 29P/30$, the angular speed of the "switched field" increases dramatically and results in significant phase lags to switch the induced poles again. Consequently, the trajectory of the chain would resume following the original field.

A nontrivial point which should also be addressed is that, the interpretation presented above mainly focuses on the global interaction between the external field and the chain based on Eq. (3). However, it is also well known that the individual particle with a permanent magnetic moment is induced to motion locally, e.g., self-spinning in a rotational field (Cebers and Ozols 2006). It is arguable if such a local motion also plays a role in the shift of trajectory. Nevertheless, the global mechanism agrees well with the experimental results in the present conditions, even without taking the local motion into consideration.

3.2 Maximum phase lags of a stable chain

According to the observations described above, it is important to record the maximum phase lag of a stable chain (denoted as $\Delta\theta_{\mathrm{Lmax}}$), so that a trajectory shift of the chain can be effectively controlled. Shown in Fig. 5 are the maximum phase lags of chains composed of different numbers of particles subjected to various perpendicular field strengths in a fixed directional field and frequency of $H_d = 24.15$ Oe and $f = 1$ Hz. The magnitudes of $\Delta\theta_{\mathrm{Lmax}}$ increase with the number of particle N as well as their perpendicular field strengths H_p, which is consistent with the early report (Li et al. 2012b). It is understandable that a longer chain induces a stronger drag, and thus leads to a larger phase lag. On the other hand, the instantaneous angular speed of the chain under a stronger field strength is much faster near the timings when the perpendicular field vanishes, so that the simultaneous phase lag is also much more significant. Nevertheless, for longer chains consisted

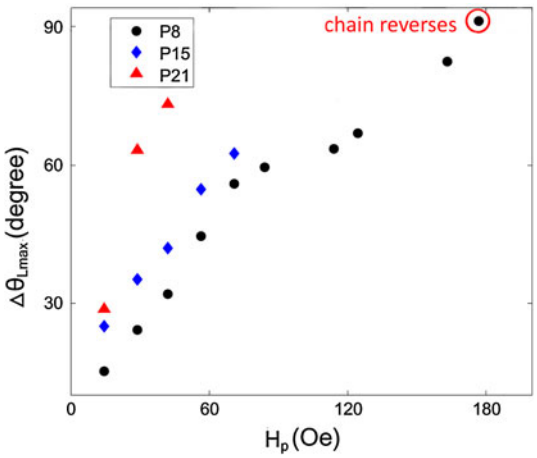

Fig. 5 Maximum instantaneous phase lag ($\Delta\theta_{\mathrm{Lmax}}$) of stable chains composed of different numbers of particles subjected to various perpendicular field strengths in a fixed directional field of $H_d = 24.15$ Oe and $f = 1$ Hz. For longer chains consisted of 15 (*P15*) and 21 (*P21*) particles, the structures are ruptured before a sufficient strong field strength can be applied to reach the condition of trajectory shift

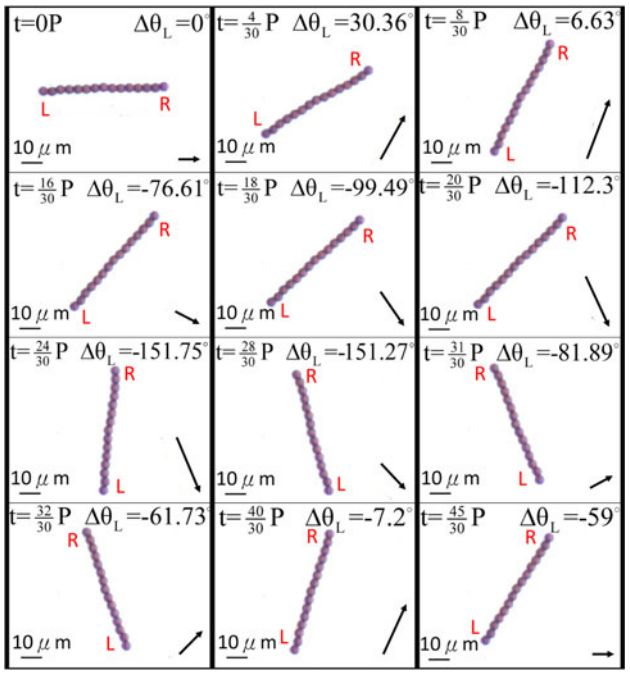

Fig. 6 Images of 15-particle (P15) chain in a weaker directional component of $H_d = 16.36$ Oe, $H_p = 42.03$ Oe, and $f = 1$ Hz. Reverse oscillation can be manipulated in a longer chain by reducing the strength of the directional field. The chain oscillates reversely along the perpendicular axis within $18P/30 < t < P$

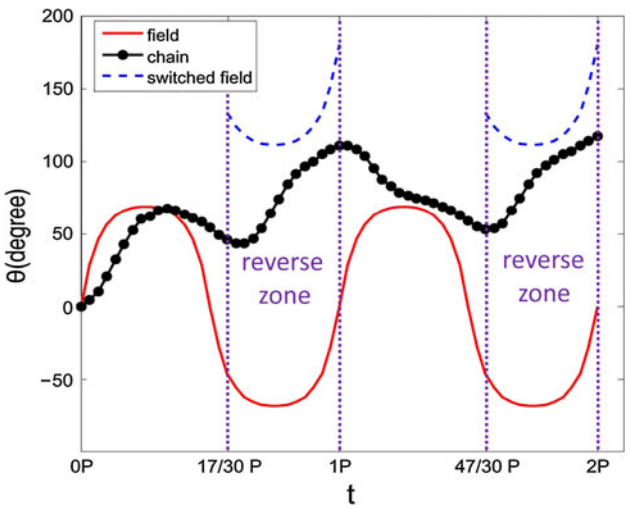

Fig. 7 Trajectories of phase angles (θ) of the external fields and the P15 chain shown in Fig. 6. Phenomenon of trajectory shift is observed. Since a longer chain leads to stronger viscous dissipation, the amplitude of oscillation of the chain is significantly smaller than both the actual input field or the imaginary "switched field"

of 15 (P15) and 21 (P21) particles, the structures are ruptured before reaching a sufficiently strong field to increase their maximum phase lags greater than 90°. It has been confirmed that the stable criterion of a oscillating chain can be determined by the dimensionless value of $N\ \mathrm{Mn}^{1/2}$

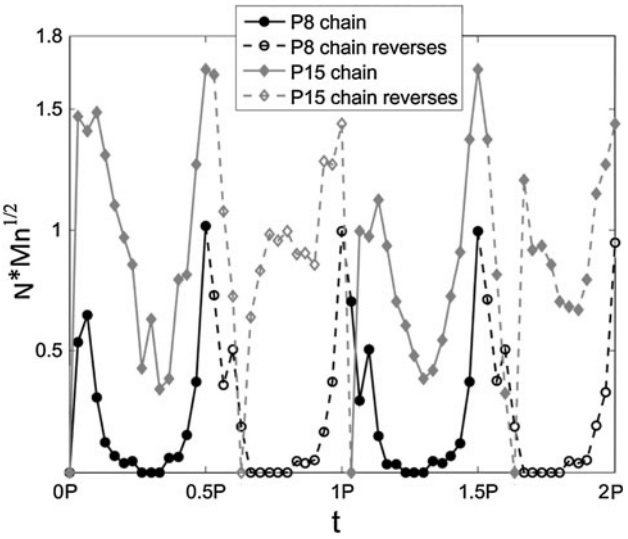

Fig. 8 Values of $N \times \mathrm{Mn}^{1/2}$ for the cases of the P8 chain and the P15 chain demonstrated in Figs. 4, 6. The values within the trajectory shift are indicated by *empty marks*. The values of $N \times \mathrm{Mn}^{1/2}$ are consistently less than 2 to ensure a stable chaining structure

(Li et al. 2012b). As a result, a possible way to increase $\Delta\theta_{\mathrm{Lmax}}$ of a chain consisted of a constant number of particles is to apply different combination of the field components, such as chaining by a weaker directional field strength. Shown in Fig. 6 are the images of a P15 chain in a weaker directional field condition of $H_d = 16.36$ Oe and subjected to $H_p = 42.03$ Oe and $f = 1$ Hz. Even the chain appears deformed slightly but remains stable due to its smaller amplitude of oscillation associated with a slower angular speed. Larger phase lags are measured throughout the oscillating period. The phase lag reaches beyond the critical magnitude of 90° at about $t = 18\mathrm{P}/30$, and starts to oscillate reversely afterward. The complete phase trajectories are plotted in Fig. 7. Similar to the forth mentioned case shown in Fig. 3, after the early stage of initial start when the chain oscillates along the horizontal axis of $\theta = 0°$, the trajectory shifts to oscillate along the perpendicular axis of $\theta = 90°$. Another feature to be noticed is the deviations of the trajectory of the chain from the external fields, both the actual field and the imaginary "switched field", in the present situation are more apparent. As discussed in Li et al. (2012b) as well as expression in Eq. (2), a longer chain leads to a stronger viscous dissipation, so that the actual amplitude of oscillation of chain would be significantly smaller than the input field.

It is also worthy to verify the stability criteria of the chaining structures in the process of reverse oscillation. The criterion of structural rupture is suggested as $N \times \mathrm{Mn}^{1/2} > 2$ (Li et al. 2012b) in the present field configuration. The correspondent values of $N \times \mathrm{Mn}^{1/2}$ within two full periods of field oscillation for the P8 (Fig. 4) and the P15 (Fig. 6) chains are shown in Fig. 8. It is found that

the maxima occur at $t = P/2$, P, 3P/2, and 2P, when the field strengths are the weakest. Besides, the maxima are all less than the critical value of two. These further verify that the chains could be effectively manipulated to oscillate reversely without ruptures.

To conclude this section, we like to emphasize that the presented experiments are carried out by applying a single kind of paramagnetic particles in a field condition of a nearly constant value of susceptibility. The influences of variation in bead susceptibility or permeability, which had been confirmed to play an important role in a rotating field (Melle and Martin 2003; Petousis et al. 2007), are not considered.

3.3 Steering of a micro-swimmer

To highlight the phenomenon of trajectory shift, it is noteworthy that such a phenomenon provides an effective manipulating mechanism to alter the motion of a magnetic chain in a MEMS. As mentioned in the previous paragraphs, the trajectory shift, which changes its oscillating axis from the horizontal axis to the perpendicular axis, can be viewed imaginary as a switch of the field orientations. In other words, the trajectory shift of a chain mimics qualitatively to the condition whose configuration of static and dynamical fields are switched. An immediate application of such a phenomenon is the steering mechanism of a micro-swimmer. As reported in Li et al. (2012a), a simple re-dispersible magnetic micro-swimmer can be constructed by connecting beads of different sizes. A representative S2L1 swimmer, which stands for a swimmer consisted of 2 small and 1 large particles, in a constant directional field condition of $H_d = 24.15$ Oe and $f = 10$ Hz is shown in Fig. 9. A perpendicular field strength of $H_p = 29.02$ Oe is initially applied till $t = 33$ s to drive the swimmer moving toward the right direction, and then increased instantly to $H_p = 163.3$Oe at $33 < t < 38.7$ s to trigger the trajectory shift and steer the swimmer upwardly. The swimmer turns counterclockwise again and moves toward the left when the perpendicular field strength is resumed to $H_p = 29.02$ Oe at $t > 38.8$ s to turn off the shift. Thus, we have successfully demonstrated that, by the presented phenomenon of trajectory shift, the micro-swimmer can be steered effectively. No physical re-configuration of the directional and dynamical fields is required.

A few more points can be addressed regarding effective manipulations of the swimmer. It is understood that the swimmer would be driven toward the direction of the center of mass along its oscillating axis, or the direction where the larger bead is located in the present condition. As a result, the driven direction of the swimmer after steering is determined by where the larger bead is pointed. In the present case shown in Fig. 9, the swimmer is turned

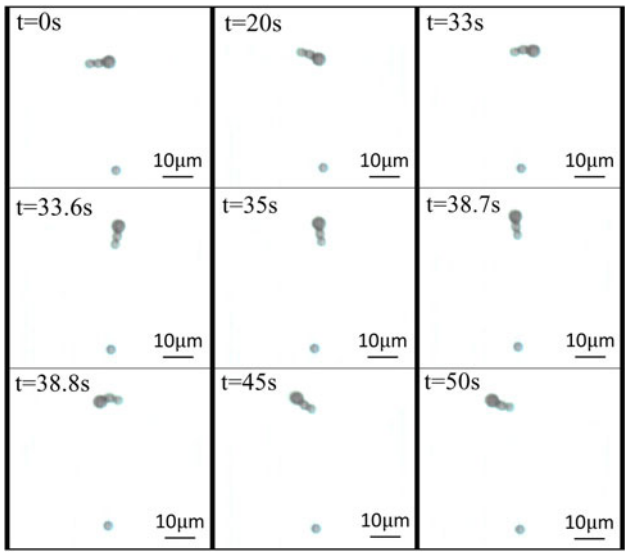

Fig. 9 Images of an S2L1 swimmer in a constant directional field strength of $H_d = 24.15$ Oe and $f = 10$ Hz. A perpendicular field strength of $H_p = 29.02$ Oe is initially applied within $t < 33$ s to drive the swimmer moving toward *right* direction, and then increased to $H_p = 163.3$ Oe at $33\text{ s} < t < 38.7$ s to turn the swimmer 90° counterclockwise and point *upwardly*. The swimmer turns counterclockwise again and moves toward the *left* at $t > 38.8$ s when the perpendicular field strength is resumed to $H_p = 29.02$ Oe. The stationary particle on the *bottom* serves as a reference position

counter-clockwise consecutively to point upwardly and left, and advances correspondently. These are achieved by varying the field strengths (or switching the field) at the timings when the lagging phase angles are negative, e.g., within the time period of $8P/30 < t < 15P/30$ of the representative case shown Fig. 2. By the same token, if a clockwise steering is desired, the switching timings should be at the timings associated with a positive magnitude of phase lag. In addition, the trajectory patterns appear to be significantly distinct between the periods of original (or chain aligning horizontally) and reverse (or chain aligning perpendicularly) oscillations, which can be clearly observed through the representative example shown in Fig. 3. As a result, the swimming effectiveness and efficiency of the swimmer moving horizontally (toward right or left) are expected to be very different from the situation moving perpendicularly (upwardly). These facts indicate that the controlling techniques to accomplish an optimal manipulation require much more dedicated studies, and are beyond the scope of the present investigation.

4 Concluding remarks

In this work, an interesting phenomenon of trajectory shift of a magnetic chain in an oscillating field is observed and experimented systematically. The trajectory shift occurs

when the phase angle difference between the oscillating chain and the external field exceeds 90°, and results in a switch of induced magnetized poles of the chain. Consequently, instead of oscillating consistently with the external field, the switch of magnetized poles leads to motion of the chain reversed to the field and oscillating along a new axis perpendicular to the original axis. Even it is apparent that the most direct factor to the trajectory shift, as expressed in Eq. (3), is the phase lag of the oscillating chain, it is noteworthy to point out that magnitudes of the phase lags are affected by many important parameters, such as strengths and configurations of the external fields as well as induced hydrodynamic drags. To manipulate such a trajectory shift, the correspondent maximum phase lags in various conditions of field strengths and number of particles consisted in the chain are investigated. Lager maximum phase lags are recorded in stronger field strengths or longer chain lengths. Nevertheless, the magnetic chain becomes unstable and ruptured if the dynamical field strength or the length of chain exceeds a certain criteria, which can be determined by a dimensionless value of $N \times \mathrm{Mn}^{1/2} < 2$. If phase shift of a longer chain is desired for the sake of its manipulations, a larger maximum phase lag can be reached by applying a weaker directional field strength to avoid a unstable rupture.

The trajectory shift provides an effective manipulating mechanism to a magnetic chain in MEMS. We have demonstrated successfully to steer micro-swimmers consisted of beads with different sizes and driven by external magnetic fields. The steering can be executed by turning on and off the trajectory shift. By the present methodology, the moving direction of micro-swimmers can be controlled even without physically re-configuring the arrangements of directional and dynamical fields.

Acknowledgments The financial support from the National Science Council of Republic of China (Taiwan) through Grant NSC 99-2221-E-009-057-MY3 is acknowledged.

References

Biswal S, Gast A (2004a) Micromixing with linked chains of paramagnetic particles. Anal Chem 76:6448–6455

Biswal S, Gast A (2004b) Rotational dynamics of semiflexible paramagnetic particle chains. Phys Rev E 69:041406

Cebers A, Ozols M (2006) Dynamics of an active magnetic particle in a rotating magnetic field. Phys Rev E 73:021505

Chen CY, Li CS (2010) Ordered microdroplet formations of thin ferrofluid layer breakups. Phys Fluids 22:014105

Chen CY, Tsai WK, Miranda JA (2008) Hybrid ferrohydrodynamic instability: coexisting peak and labyrinthine patterns. Phys Rev E 77:056306

Chen CY, Yang YS, Miranda JA (2009) Miscible ferrofluid patterns in a radial magnetic field. Phys Rev E 80:016314

Chen CY, Wu WL, Miranda JA (2010) Magnetically induced spreading and pattern selection in thin ferrofluid drops. Phys Rev E 82:056321

Dreyfus R, Baudry J, Roper ML, Fermigier M, Stone HA, Bibette J (2005) Microscopic artificial swimmers. Nature 437:862

Ghosh A, Fischer P (2009) Controlled propulsion of artificial magnetic nanostructured propellers. Nano Lett 9(6):2243–2245

Gijs M (2004) Magnetic bead handling on-chip: new opportunities for analytical application. Microfluid Nanofluid 1:22–40

Kang TG, Hulsen M, Anderson P, den Toonder J, Meijer H (2007) Chaotic mixing induced by a magnetic chain in a rotating magnetic field. Phys Rev E 76:066303

Karle M, Wohrle J, Miwa J, Paust N, Roth G, Zengerle R, von Stetten F (2011) Controlled counter-flow motion of magnetic bead chains rolling along microchannels. Microfluid Nanofluid 10:935–939

Kodama S (2008) Dynamic ferrofluid sculpture: organic shape-changing art forms. Commun ACM 51:79

Lacharme F, Vandevyver C, Gijs MAM (2009) Magnetic beads retention device for sandwich immunoassay comparison of off-chip and on-chip antibody incubation. Microfluid Nanofluid 7:479–487

Li YH, Sheu ST, Pai JM, Chen CY (2012a) Manipulations of oscillating micro magnetic particle chains. J Appl Phys 111:07A924

Li YH, Chen CY, Sheu ST, Pai JM (2012b) Dynamics of a microchain of superparamagnetic beads in an oscillating field. Microfluid Nanofluid 13:579–588

Martin J, Shea-Roher L, Solis K (2009) Strong intrinsic mixing in vortex magnetic fields. Phys Rev E 80:016312

Melle S, Martin J (2003) Chain model of a magnetorheological suspension in a rotating field. J Chem Phys 118(21):9875

Melle S, Fuller G, Rubio M (2000) Structure and dynamics of magnetorheological fluids in rotating magnetic fields. Phys Rev E 61(4):4111–4117

Melle S, Calderon O, Fuller G, Rubio M (2002a) Polarizable particle aggregation under rotating magnetic fields using scattering dichroism. J Colloid Interface Sci 247:200

Melle S, Calderon O, Rubio M, Fuller G (2002b) Rotational dynamics in dipolar colloidal suspensions: video microscopy experiments and simulations results. J Non-Newton Fluid Mech 102(2):135–148

Melle S, Calderon O, Rubio M, Fuller G (2003) Microstructure evolution in magnetorheological suspensions governed by Mason number. Phys Rev E 68:041503

Nguyen NT (2012) Micro-magnetofluidics: interactions between magnetism and fluid flow on the microscale. Microfluid Nanofluid 12:1–16

Petousis I, Homburg E, Derks R, Dietzel A (2007) Transient behaviour of magnetic micro-bead chains rotating in a fluid by external fields. Lab Chip 7:1746

Rosensweig RE (1985) Ferrohydrodynamics. Cambridge University Press, Cambridge

Roy T, Sinha A, Chakraborty S, Ganguly R, Puri I (2009) Magnetic microsphere-based mixers for microsroplets. Phys Fluids 21:027101

Terray A, Oakey J, Marr D (2002) Microfluidic control using colloidal devices. Science 296:1841–1844

Vuppu A, Garcia A, Hayes M (2003) Video microscopy of dynamically aggregated paramagnetic particle chains in an applied rotating magnetic field. Langmuir 19:8646

Weddemann A, Wittbracht F, Auge A, Hutten A (2011) Particle flow control by induced dipolar interaction of superparamagnetic microbeads. Microfluid Nanofluid 10:459–463

Wittbracht F, Weddemann A, Eickenberg B, Hutten A (2012) On the direct employment of dipolar particle interaction in microfluidic system. Microfluid Nanofluid 13:543–554